



## The ( $e^+ + e^-$ ) flux measurement up to 1 TeV with the AMS-02 experiment

V. Vagelli<sup>a</sup>, Z.L. Weng<sup>b</sup>, on behalf of the AMS-02 Collaboration

<sup>a</sup>*Institut für Experimentelle Kernphysik, Karlsruhe Institute of Technology, KIT, D-76128 Karlsruhe, Germany*

<sup>b</sup>*Massachusetts Institute of Technology, MIT, Cambridge, MA 02139, USA*

---

### Abstract

AMS-02 is a large acceptance cosmic ray detector operating on the International Space Station since May 2011. Of the  $\sim 41$  billion events collected in the first 30 months of data taking, 10.6 million have been selected as  $e^+$  and  $e^-$  for the measurement of the ( $e^+ + e^-$ ) energy spectrum from 0.5 GeV to 1 TeV. In this contribution, the latest result on the ( $e^+ + e^-$ ) flux measurement with AMS is presented.

**Keywords:** AMS, Cosmic Rays, Electrons, Positrons.

---

The measurement of the positrons and electrons ( $e^\pm$ ) in cosmic rays provides fundamental information about the origin and the propagation of  $e^\pm$  in the galaxy. Recent measurements of the positron fraction, of the  $e^+$  flux up to 500 GeV, and of the  $e^-$  flux up to 700 GeV by the Alpha Magnetic Spectrometer (AMS) [1, 2] have confirmed the existence of an additional  $e^\pm$  source at high energies beyond well established astrophysical mechanisms. The AMS measurements of  $e^+$  and  $e^-$  are discussed in [3]. This contribution discusses the AMS measurement of the ( $e^+ + e^-$ ) cosmic ray flux from 0.5 GeV to 1 TeV, based on the analysis presented in [4].

### 1. AMS detector

AMS is a general purpose high-energy particle physics detector which has been installed on the International Space Station in May 2011 to conduct a unique long-duration ( $\sim 20$ -year) mission of fundamental physics research in space. The AMS detector is fully described in [5].

The core of AMS consists of a tracker and a 0.14 T permanent magnet. Nine planes of double-sided silicon microstrip tracker measure the coordinates and energy losses of cosmic rays in each plane to determine their trajectory and absolute charge,  $|Z|$ . The tracker measures the particle rigidity  $R = p/Z$ , where  $p$  is the mo-

mentum, over a lever arm of 3 m. The maximum detectable rigidity is 2 TV.

Four Time Of Flight (TOF) planes trigger the readout of the detector and measure the particle velocity and flight direction. The curvature measured with the tracker and the flight direction of the particle measured with the TOF yield the sign of the charge. Particles outside the geometric acceptance are rejected by anti-coincidence counters located inside the magnet bore with inefficiency less than  $10^{-5}$ .

The AMS detector is completed by a ring imaging Cherenkov detector, an electromagnetic calorimeter (ECAL), and a transition radiation detector (TRD). The tracker, TOF, and TRD each measure  $|Z|$  independently.

The 3-dimensional imaging capability of the 17 radiation length ( $17 X_0$ ) ECAL provides an accurate measurement of the shower shape and of the  $e^\pm$  energy scaled to the top of AMS ( $E$ ). An ECAL estimator, based on a boosted decision tree algorithm [6], is used to differentiate  $e^\pm$  from protons by exploiting their different shower shapes.

To further differentiate between  $e^\pm$  and protons, the signals from the 20 layers of proportional tubes in the TRD are combined into a TRD classifier formed from the product of the probabilities of the  $e^\pm$  hypothesis.

More details about the AMS  $e^\pm$  identification capabilities are covered in [7].

## 2. Analysis

AMS collected  $\sim 41$  billion events from 19 May 2011 to 26 Nov. 2013. The data have been analyzed to measure the isotropic  $\Phi(e^+ + e^-)$  flux, defined as:

$$\Phi(e^+ + e^-) = \frac{N(E)}{A(E) \cdot \epsilon_T(E) \cdot \epsilon_E(E) \cdot T(E) \cdot \Delta E} \quad (1)$$

where  $N$  is the number of  $(e^+ + e^-)$  events,  $A$  is the effective detector acceptance,  $\epsilon_T$  is the trigger efficiency,  $\epsilon_E$  is the ECAL signal selection efficiency and  $T$  is the exposure time.

$\Phi(e^+ + e^-)$  has been measured in 74 independent energy bins of width  $\Delta E$  from 0.5 GeV to 1 TeV. The bin width amounts to at least 2 times the ECAL resolution, and it smoothly increases with energy to ensure enough data in each bin. The bin-to-bin migration effect due to the finite ECAL resolution is  $\sim 1\%$  at 1 GeV and it decreases down to 0.2% above 10 GeV. Its contribution to the total measurement systematic uncertainty is found to be negligible if compared with other systematic effects discussed below.

The absolute energy scale is verified on data collected in space by the comparison of minimum ionizing particle signals and of the ratio  $E/p$  with test beam values. The scale is known with a precision of 2% in the test beam range [10, 290] GeV. The uncertainty increases up to 5% at 0.5 GeV and at 1 TeV. This is assigned as uncertainty to the energy bin boundaries.

Downward-going relativistic particles with a single reconstructed tracker track crossing at least 8 of the 20 TRD layers and passing through the ECAL are selected for the analysis. Particles with  $|Z| > 1$  are rejected using  $dE/dx$  in the tracker and in the TRD. Particles that only ionize in the first  $5X_0$  of the ECAL are rejected. Secondary particles of atmospheric origin [8] are rejected with the cutoff requirement discussed below.

The sample purity is enhanced by a selection on the ECAL classifier. Its efficiency,  $\epsilon_E$ , is measured from the data using negative charge sign samples. Optimal  $\epsilon_E$  values range from 75% to 95% depending on the number of signal and background events in the energy bin.

The amount of  $(e^+ + e^-)$  events is finally evaluated using a data-driven approach. TRD classifier reference spectra, or *templates*, for  $(e^+ + e^-)$  and for protons are fitted to the selected sample varying their normalization in each energy bin. This procedure provides the yield of  $(e^+ + e^-)$  events,  $N$ , and the statistical uncertainty on  $N$  and on the number of background events. The statistical fluctuations dominate the measurement uncertainty above  $\sim 200$  GeV. The template fit result in the [149, 170] GeV energy bin is shown for reference in

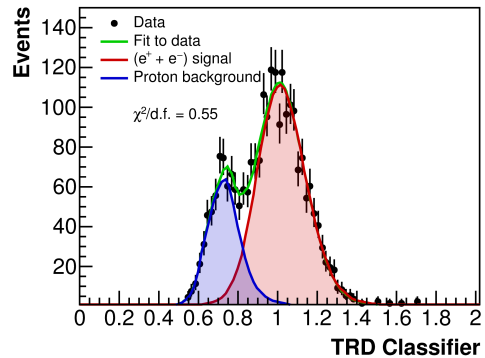


Figure 1: Result of the template fit in the [149, 170] GeV energy bin.

Figure 1. A total of 10.6 million  $(e^+ + e^-)$  events have been identified with energies from 0.5 GeV to 1 TeV. The number of events corrected by the ECAL selection efficiency is calculated as  $N_E = N/\epsilon_E$ .

The templates for the  $(e^+ + e^-)$  signal and for the proton background are constructed from the data, separately in each bin, using pure samples of  $e^-$  and protons. The signal template does not show any energy dependence above  $\sim 10$  GeV. Therefore, all the  $e^-$  selected with high purity in the [15.1, 83.4] GeV energy range are used to define a unique signal template up to the highest energies. The systematic uncertainty on  $N_E$  is defined by the level of accuracy to which the template shapes and  $\epsilon_E$  are known. To evaluate this, the complete analysis has been performed 2000 times in each energy bin. For each trial, different ECAL estimator cuts and different selections, which are used to define the templates from the data, have been tested. The ECAL estimator selection has been varied in an interval of  $\pm 5\%$  in efficiency around the value of the cut that minimizes the combined statistical and systematic uncertainties. The stability of the result for all the trials quantifies the systematic uncertainty of  $N_E$ . This is the main source of systematic uncertainty above  $\sim 500$  GeV.

A Monte Carlo (MC) program based on the Geant 4.9.4 package [9] is used to simulate physics processes and detector signals. The acceptance for a particle that passes through the AMS active volumes is evaluated using the MC simulation and it amounts to  $\sim 550$  cm<sup>2</sup> sr. The event selection efficiency amounts to 90% at 10 GeV, 83% at 100 GeV, and 70% at 1 TeV. The acceptance is corrected by the minor differences observed between the data and the MC simulation. This correction is a smooth, slowly varying function of energy. It is -4% at 10 GeV and -3% at 1 TeV. The uncertainty on the acceptance amounts to 2% above 3 GeV and does not show any strong energy dependence. It

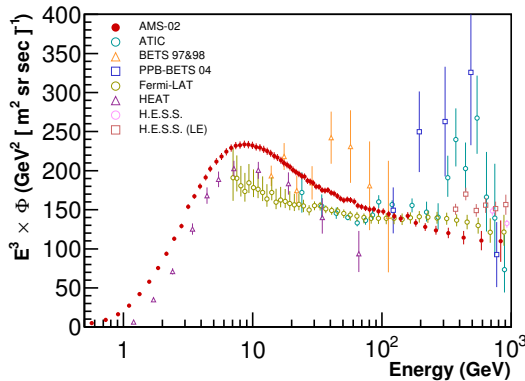


Figure 2:  $\Phi(e^+ + e^-)$  measured by AMS multiplied by  $E^3$ . The AMS error bars are the quadratic sum of the statistical and systematic errors. The results from earlier experiments [11, 12, 13, 14, 15, 16, 17] are also shown.

dominates the measurement systematic uncertainty below  $\sim 500$  GeV.

The trigger efficiency,  $\epsilon_T$ , is determined from data using a dedicated, unbiased trigger stream. It is measured to be 100% above 3 GeV decreasing to 75% at 1 GeV.

The exposure time  $T$  is calculated for each energy bin by the sum of livetime-weighted seconds of data taking. The seconds are added up only if the minimum energy of the bin exceeds 1.2 times the maximum Størmer cutoff [10] for  $|Z|=1$  particles in the AMS geometric acceptance. The exposure time amounts to  $6.2 \times 10^7$  s above 30 GeV and it decreases below 30 GeV due to the non-negligible effect of the geomagnetic cutoff.

### 3. Result

The  $(e^+ + e^-)$  flux, calculated according to Equation 1 and multiplied by  $E^3$ , is presented in Figure 2 together with previous measurements. Below  $\sim 10$  GeV, the behavior of  $\Phi(e^+ + e^-)$  is affected by solar modulation. Above 20 GeV the effects of solar modulation are insignificant within the current experimental accuracy.

The data show no relevant feature and the flux is smooth above 10 GeV. The flux can be described by a single power law ( $\Phi \propto E^\gamma$ ) above 30 GeV. The result of the single power law fit to  $\Phi(e^+ + e^-)$  is shown as the black dashed line in Figure 3. The existence of a prominent spectral feature above 300 GeV is excluded. Other possible spectral anomalies are strongly constrained. The flux measured by AMS results softer than previous measurements at high energies. More details about the analysis of the energy dependence of  $\Phi(e^+ + e^-)$  are discussed in [4].

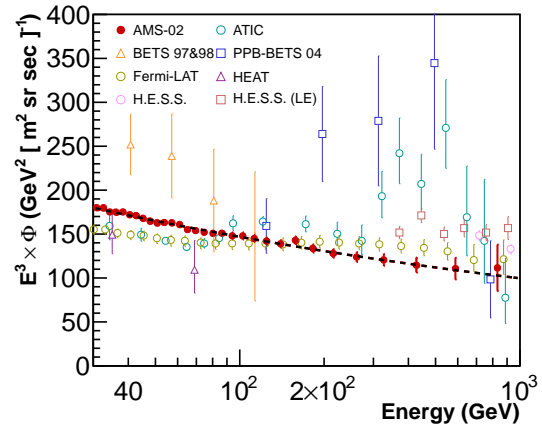


Figure 3: Single power law fit (dashed black line) to the  $\Phi(e^+ + e^-)$  AMS measurement.

In conclusion, the redundant  $e^\pm$  identification capabilities and the accurate energy measurement of AMS provide high quality data for the measurement of  $e^\pm$  in cosmic rays. The precision measurement by AMS shows that the  $(e^+ + e^-)$  flux is smooth up to 1 TeV and no prominent features in the spectrum are observed.

### Acknowledgments

This work has been supported by persons and institutions acknowledged in [1, 2, 5].

### References

- [1] L. Accardo *et al.*, Phys. Rev. Lett. **113** (2014) 121101.
- [2] M. Aguilar *et al.*, Phys. Rev. Lett. **113** (2014) 121101.
- [3] Z. L. Weng *et al.*, These proceedings, **673**.
- [4] M. Aguilar *et al.*, accepted for publication in Phys. Rev. Lett.
- [5] M. Aguilar *et al.*, Phys. Rev. Lett. **110** (2013) 141102.
- [6] B. Roe *et al.*, Nucl. Instr. Meth. **A 543** (2005) 577.
- [7] M. Graziani, These proceedings, **821**.
- [8] J. Alcaraz *et al.*, Phys. Lett. **B 484** (2000) 10.
- [9] J. Allison *et al.*, IEEE Trans. Nucl. Sci. **53** (2006) 270; S. Agostinelli *et al.*, Nucl. Instrum. Meth. **A 506** (2003) 250.
- [10] D. Smart and M. Shea, Adv. Sp. Res. **36** (2005) 2012; C. Størmer, The Polar Aurora, Oxford University Press, London (1950).
- [11] S. Torii *et al.*, Astrophys. J. **559**, 973 (2001).
- [12] M. A. DuVernois *et al.*, Astrophys. J. **559** (2001) 296.
- [13] J. Chang *et al.*, Nature (London) **456**, 362 (2008).
- [14] K. Yoshida *et al.*, Advances in Space Research **42**, 1670 (2008).
- [15] F. Aharonian *et al.*, Phys. Rev. Lett. **101** (2008) 261104.
- [16] F. Aharonian *et al.*, Astron. Astrophys. **508** (2009) 561.
- [17] M. Ackermann *et al.*, Phys. Rev. **D 82** (2010) 092004.